Performance of MIMO Enhanced Unipolar OFDM with Realistic Indoor Visible Light Channel Models

Anil Yesilkaya*, Farshad Miramirkhani†, Ertugrul Basar ‡, Erdal Panayirci* and Murat Uysal†
* Kadir Has University, Istanbul, Turkey
Email: { anil.yesilkaya, eepanay }@khas.edu.tr
† Ozyegin University, Istanbul, Turkey
Email: { farshad.miramirkhani, murat.uysal }@ozyegin.edu.tr
‡ Istanbul Technical University, Istanbul, Turkey
Email: basarer@itu.edu.tr

***Abstract*—Visible light communication (VLC) involves the dual use of illumination infrastructure for high speed wireless access. Designing such optical based communication systems, realistic indoor optical channel modeling becomes an important issue to be handled. In this paper, first we obtain new realistic indoor VL channel characterizations and models, in a multiple-input multiple-output (MIMO) transmission scenario, using non-sequential ray tracing approach for the channel impulse responses (CIRs). Practical issues such as number of light emitting diode (LED) chips per luminary, spacing between LED chips, objects inside the room and cabling topology are also investigated. On the other hand, since indoor optical channels exhibit frequency selectivity, multi-carrier communication systems, particularly orthogonal frequency division multiplexing (OFDM) is used to handle the resulting inter-symbol interference in VLC systems. Hence, we propose a new MIMO-OFDM based VLC system, called MIMO enhanced unipolar OFDM (MIMO-eU-OFDM) by combining MIMO transmission techniques with the recently proposed eU-OFDM scheme. The bit error rate (BER) performance of the proposed system is investigated in the presence of the 2×2 and 4×4 realistic MIMO VLC channels and its BER performance is compared with the reference optical MIMO-OFDM systems.**

***Index Terms*—Optical wireless communication (OWC), MIMO enhanced unipolar orthogonal frequency division multiplexing (MIMO-eU-OFDM), realistic indoor MIMO-VLC channel modeling.**

I. Introduction

Optical wireless communications (OWC) is an up and coming technology to complement wireless radio frequency (RF) systems. OWC comprises VL (visible light) and IR (infra red) regions of the spectrum as indoor/outdoor wireless communications medium. Visible light communications (VLC) is a branch of OWC operating in the (390-750nm) band and providing number of advantages over RF and millimeter wave communications. VLC is a not complex, expensive or scarce technology. It offers almost 10.000 times larger unregulated and RF non-interfering spectrum with improved data security [1]. Moreover, it could be realized by off-the-shelf components which allow to reuse of the existing lightning infrastructure. Therefore, VLC enables secure and free of health concern transmission where RF and millimeter wave communications are physically impossible or prohibited. Recent developments in light emitting diode (LED) manufacturing technologies are leading innovations in solid state lighting (SSL) as a source of illumination while LED's are starting to replace the incandescent and fluorescent lighting. LED's can be modulated at rates several hundred times that of incandescent and fluorescent light sources in such a power efficient way [2]. Intensity Modulation/Direct Detection (IM/DD) is the most practical modulation technique to use in indoor VLC. In IM/DD technique, information is carried by the intensity of the light. Then at the receiver, fluctuations in the intensity converted to electrical signal. Therefore, the signal carrying information by the IM/DD system should be real and non-negative valued. Implementation of the orthogonal division multiplexing (OFDM) signaling employed in IM/DD systems has showed great promise in terms of spectral efficiency and robustness against inter-symbol interference (ISI) [3].

Many of the recent works about optical OFDM (O-OFDM) systems have revealed the fact that each scheme has strengths and weaknesses in different metrics. DC-biased optical OFDM (DCO-OFDM) suffers from poor average optical efficiency. Power efficient asymetrically clipped optical OFDM (ACO-OFDM) suffers from loss of half degrees of freedom (e.g., spectral efficiency) [4]. Unipolar OFDM, which neither requires DC biasing nor asymmetrically clipping, has been proposed as an alternative to DCO-OFDM and ACO-OFDM techniques [5]. However, the spectral efficiency of U-OFDM is half of DCO-OFDM, which makes the U-OFDM scheme power inefficient for higher order modulations. Recently, enhanced U-OFDM (eU-OFDM) scheme has been proposed in [6], which utilizes the positive and negative separated frame structure of the U-OFDM and allows multiple U-OFDM information streams superimposed on top of each other in order to not sacrifice from the spectral efficiency. Due to its advantages in terms of power and spectral efficiency, eU-OFDM appears as a strong alternative for future OWC standards. On the other hand, considering the advantages of inherently available multiple-input-multiple-output (MIMO) optical wireless systems, the combination of the aforementioned optical OFDM techniques with MIMO transmission is inevitable [7].

Despite the recent surge of interest in VLC mentioned

This work is supported by COST-TUBITAK Research Grant No: 113E307.

This work is carried out as an activity of Centre of Excellence in Optical Wireless Communication Technologies (OKATEM) funded by Istanbul Development Agency (ISTKA) under Innovative Istanbul Financial Support Program, 2015. The statements made herein are solely the responsibility of the authors and do not reflect the views of ISTKA and/or T.R. Ministry of Development.

978-1-4673-8666-1/16/$31.00 ©2016 IEEE

above, a lot of research problems related modeling of the VLC channel model and performance of the optical modulations schemes in various models still remain open. This work first presents realistic channel models for MIMO VLC systems by considering geometry of the environment, objects inside, the reflection characteristics of the materials as well as the specifications of the sources and receivers by using non-sequential ray tracing approach. The obtained channel impulse responses (CIR's) for MIMO scenario comprises practical issues such as number of LED chips per luminary, spacing between LED chips, objects inside the room and wiring topology. Second, by combining MIMO and eU-OFDM techniques, a new optical OFDM scheme, called MIMO-eU-OFDM, is proposed in this study. The bit error rate (BER) performance of MIMO-eU-OFDM is studied by computer simulations in the presence of 2×2 and 4×4 realistic MIMO VLC channel models and its BER performance is compared with the reference optical MIMO-OFDM systems.

The rest of the paper is organized as follows: In Section II, we briefly summarize the channel modeling approach. In Section III, we describe the MIMO-eU-OFDM system under consideration. In Section IV, we present simulation results for the BER performance evaluation of MIMO-eU-OFDM. Finally, we conclude the paper in Section V.

II. Realistic VLC Channel Modeling

We now present a novel and realistic channel modeling approach for VLC that overcomes the limitations of previous works. Our study is based on Zemax® which is an optical illumination design software with sequential and non-sequential ray-tracing capabilities [8]. With an accurate description of interactions among rays emitted from the LEDs in a user defined environment, the non-sequential ray-tracing is based on tracing the rays along physically realizable paths until they intercept an object. Wavelength dependency, effect of realistic light sources as well as different types of reflections are taken into consideration. Non-sequential ray tracing algorithms allow us to calculate the detected power and path lengths from source to detector for each ray. These are then processed to yield the channel impulse responses (CIRs) for various indoor environments. The line-of-sight (LOS) response depends on the LOS distance. Besides the LOS component, there is a large number of reflections from the ceiling, walls, floor and as well as objects within the environment.

In this paper, we particularly focus on a specific MIMO scenario where four luminaries and four detectors are placed on the ceiling and on the table (besides the laptop e.g., USB device) respectively. We present the channel modeling with practical considerations such as number of LED chips per luminary, objects inside the room and cabling topology. After the evaluation of CIRs, we also investigate the effect of the propagation delay of cables on the CIRs. We show that a sparse channel model is obtained as a result of wiring topology of communication access point to luminaries. This type of channel model arises in indoor VLC systems such as homes and offices normally using multiple LED luminaries. Two important issues to modeling of the channel for these environments are number of LED chips and distance between them in each luminary. In fact, the number of LEDs and spacing between them affect the channel parameters such as channel DC gain, root mean square (RMS) delay spread and mean excess delay spread which are used in MIMO systems. However, the only channel models for MIMO VLC systems presented in literature [3], [4] are obtained by unrealistic conditions such as fixed reflectance for materials, ideal Lambertian pattern for LEDs and by considering empty room.

We now investigate some realistic indoor channel models and generate their CIRs for MIMO VLC systems consisting of 4 transmit and 4 receive units. The CIRs obtained with the ray tracing method of Zemax® software also enables us to specify the objects located in and the geometry of an indoor as well as the reflection characteristics of the surface materials, specifications of the sources (i.e., LEDs) and receivers (i.e., photodiodes) [9]–[11]. We consider a room size of $5 \times 5 \times 3$ meters (see Fig. 1) with single user - 4 transmit and 4 receive units. In [12], an ideal case has been considered in which 100 LED chips per each luminary were employed. However, by a simplifying technique, we can put lesser number of LED chips in each luminary to achieve the same channel parameters [13]. We place four luminaries on the ceiling, each consisting of 9 LED chips with spacing of 30 cm. Each LED chip radiates 5 W with a view angle of 120°. The field of view (FOV) and the area of the detector are 85°and 1 cm^2, respectively. Four detectors placed on the desk at a height of 80 cm (standard desk height) with equal distances between them (10 cm). The materials of the walls, ceiling, floor, desk, chair and laptop are plaster, plaster, pine wood, pine wood, black gloss paint and black gloss paint [10]. The user is located in a symmetrical position with respect to the transmit units. Additionally, the locations of receiver units placed on the table are randomly selected. In Table I, different parameters of our configuration are given for a MIMO VLC system.

TABLE I: Channel Configurations

Parameters	Values
Size of room (m)	$5 \times 5 \times 3$
Number of luminaries	4
Number of chips per luminary	9
Model of each chip	Cree Xlamp® MC-E
Power of each chip	5 W
Luminary positions (m)	(1.3, 0.7, 3) (1.3, -1.3, 3) (-0.7, -1.3, 3) (-0.7, 0.7, 3)
Photodetector (PD) positions	(-0.14, -0.5, 0.8) (-0.14, -0.4, 0.8) (-0.14, -0.5, 0.8) (-0.14, -0.4, 0.8)
View angle of luminary	120°
FOV of PD	85°
Area of PD	1 cm^2
Materials (Wavelength dependent reflectance)	Walls: Plaster, Ceiling: Plaster Floor: Pine wood, Desk: Pine wood Chair: Black gloss paint Laptop: Black gloss paint

The three different indoor MIMO-VLC configurations considered in this paper for channel modeling are shown in Fig. 1. Power delay profiles of each channel (totally 16 channels exist) and their frequency responses are presented in Figs. 2 and 3, respectively. Table II presents the channel parameters of the CIRs between each luminary and each detector. The entire luminaries are assumed to emit light simultaneously. Obviously, all luminaries may not emit light at the same instant because of the difference of wiring topology. Therefore, this fact should be taken into consideration while a channel model is constructed in its general form. As shown in Fig. 4, the signal travels

The CIRs obtained for typical home, office and factory environments through our approach were accepted as reference VLC channel models by the ongoing VLC standardization group IEEE802.15.7r.

M. Uysal, T. Baykas, F. Miramirkhani, and et.al, TG7r1 channel model document for high-rate PD communications.

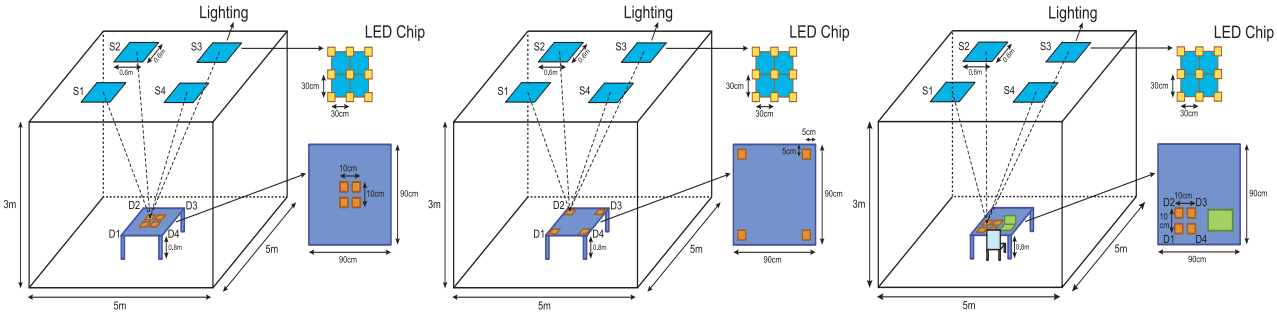

Fig. 1: Configuration A (receivers located in center), B (receivers located in corners) and C (receivers at the left corner, chair and laptop exists)

TABLE II: Channel parameters for configurations A, B and C

	Configuration A (receivers located in center, $d_{RX} = 0.1$)				**Configuration B (receivers located at corners, $d_{RX} = 0.8$)**				**Configuration C (receivers at the left corner, chair and laptop exists)**			
Channel	T_{tr} $[ns]$	τ_0 $[ns]$	τ_{RMS} $[ns]$	H_0	T_{tr} $[ns]$	τ_0 $[ns]$	τ_{RMS} $[ns]$	H_0	T_{tr} $[ns]$	τ_0 $[ns]$	τ_{RMS} $[ns]$	H_0
$h_{1,1}$	40	14.22	10.18	2.17×10^{-4}	37	12.40	8.98	2.94×10^{-4}	39	13.27	9.48	2.46×10^{-4}
$h_{1,2}$	40	14.44	9.79	2.19×10^{-4}	40	15.22	10.40	1.78×10^{-4}	40	13.83	9.90	2.04×10^{-4}
$h_{1,3}$	40	14.52	9.84	2.04×10^{-4}	42	17.28	11.23	1.38×10^{-4}	38	13.23	9.27	2.28×10^{-4}
$h_{1,4}$	40	14.44	9.79	2.19×10^{-4}	40	15.22	10.40	1.78×10^{-4}	39	14.07	9.77	2.02×10^{-4}
$h_{2,1}$	40	14.44	9.79	2.19×10^{-4}	40	15.22	10.40	1.78×10^{-4}	41	16.56	10.73	1.52×10^{-4}
$h_{2,2}$	40	14.22	10.18	2.17×10^{-4}	37	12.40	8.98	2.94×10^{-4}	41	17.20	11.04	1.33×10^{-4}
$h_{2,3}$	40	14.44	9.79	2.19×10^{-4}	40	15.22	10.40	1.78×10^{-4}	40	15.67	10.28	1.55×10^{-4}
$h_{2,4}$	40	14.52	9.84	2.04×10^{-4}	42	17.28	11.23	1.38×10^{-4}	42	17.99	11.44	1.12×10^{-4}
$h_{3,1}$	40	14.52	9.84	2.04×10^{-4}	42	17.28	11.23	1.38×10^{-4}	40	14.51	9.96	1.92×10^{-4}
$h_{3,2}$	40	14.44	9.79	2.19×10^{-4}	40	15.22	10.40	1.78×10^{-4}	41	15.64	10.63	1.60×10^{-4}
$h_{3,3}$	40	14.22	10.18	2.17×10^{-4}	37	12.40	8.98	2.94×10^{-4}	40	15.15	10.52	1.64×10^{-4}
$h_{3,4}$	40	14.44	9.79	2.19×10^{-4}	40	15.22	10.40	1.78×10^{-4}	40	14.91	10.25	1.74×10^{-4}
$h_{4,1}$	40	14.44	9.79	2.19×10^{-4}	40	15.22	10.40	1.78×10^{-4}	37	11.73	8.64	3.32×10^{-4}
$h_{4,2}$	40	14.52	9.84	2.04×10^{-4}	42	17.28	11.23	1.38×10^{-4}	37	12.01	8.56	3.29×10^{-4}
$h_{4,3}$	40	14.44	9.79	2.19×10^{-4}	40	15.22	10.40	1.78×10^{-4}	37	11.79	8.56	3.10×10^{-4}
$h_{4,4}$	40	14.22	10.18	2.17×10^{-4}	37	12.40	8.98	2.94×10^{-4}	38	11.99	8.85	2.90×10^{-4}

from communication access point to the luminary (array of LED chips) through a wired connection. Based on the simulation parameters, we used four luminaries on top of the ceiling where the dimensions of room is $5 \times 5 \times 3$ meters. Fig. 5 illustrates the wiring topology for our indoor environment model where a CAT-5 cable by length of 2 m between each luminary is employed [14]. This cable introduces a propagation delay of 5 nsecs per meter. Fig. 6 depicts the artificial multipath CIR as seen at the receiver (D1) taking into account the delays caused by cabling (see Fig. 5). Fig. 6 shows the CIR including the delays caused by cabling. We observe that the CIR, obtained in Fig. 6 exhibits a sparse channel model as a result of the wiring between luminaries in indoor VLC.

III. MIMO Enhanced Unipolar OFDM (MIMO-eU-OFDM) System

U-OFDM [5] has been proposed as an alternative to ACO-OFDM and DCO-OFDM techniques and it neither requires AC nor DC biasing for the operation of optical OFDM. U-OFDM scheme provides an unique solution for the transformation of bipolar OFDM signals obtained after IFFT operation to unipolar signals for their transmission over optical wireless links. In U-OFDM scheme, each bipolar frame is split into two unipolar frames (one positive and one negative frame), and these frames are transmitted one by one. According to U-OFDM principle a bipolar frame as

$$\mathbf{x} = [-1.2 \quad 4.2 \quad 3.5 \quad -2.3] \tag{1}$$

can be transformed into

$$\mathbf{x} = [\mathbf{x}_P \quad \mathbf{x}_U] = [0 \quad 4.2 \quad 3.5 \quad 0 \quad 1.2 \quad 0 \quad 0 \quad 2.3] \tag{2}$$

where $\mathbf{x}_P$ and $\mathbf{x}_U$ denote the corresponding positive and negative frame, respectively. At the receiver side, the original bipolar frame can be obtained by subtracting the negative frame from the positive frame. The major drawback of the U-OFDM scheme is its reduced spectral efficiency given as,

$$\eta_U = \frac{\log_2(M)(N_{FFT}-2)}{4N_{FFT}} \approx \frac{\log_2(M)}{4} \tag{3}$$

which is the half of the DCO-OFDM. In (3), M is the size of the considered M-QAM constellation, and N_{FFT} is the FFT size. The factor of $1/4$ comes from the combined effects of Hermitian symmetry and doubling the frame size with positive/negative frames.

eU-OFDM scheme [6], [15] is obtained by the modification of the U-OFDM scheme to achieve a higher spectral efficiency. eU-OFDM scheme doubles the spectral efficiency of U-OFDM and obtains the same spectral efficiency as that of DCO-OFDM by combining several U-OFDM frames in a clever way. Fig. 7 shows the signal generation of eU-OFDM for $L = 3$ layers. As seen from Fig. 7, for the implementation of eU-OFDM scheme, 2^{L-l} bipolar OFDM frames are generated for each layer $l = 1, 2, \ldots, L$. Then, these frames are transformed into unipolar frames by U-OFDM principle, where $P_{l,k}$

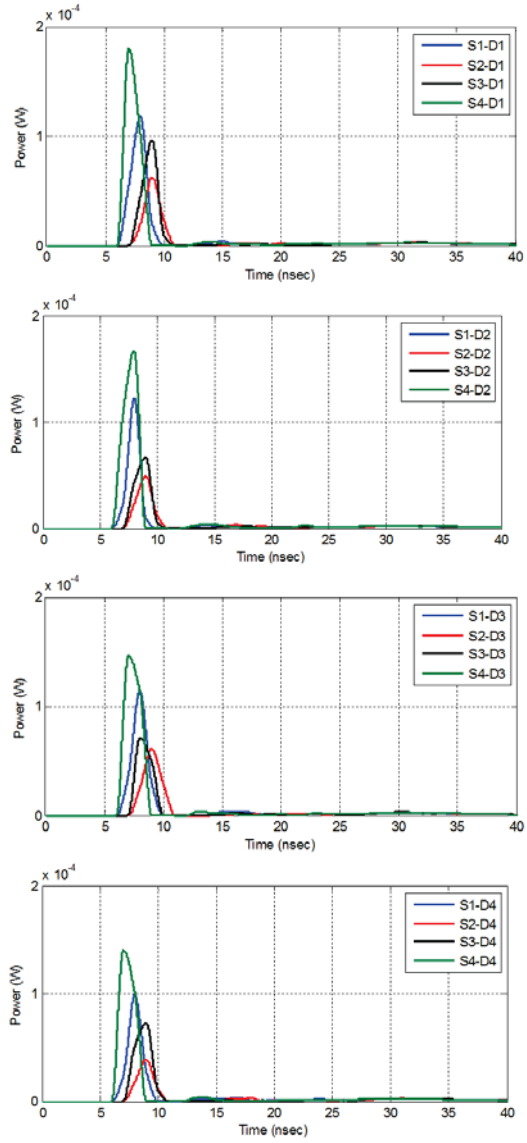

Fig. 2: The PDP's for configuration C

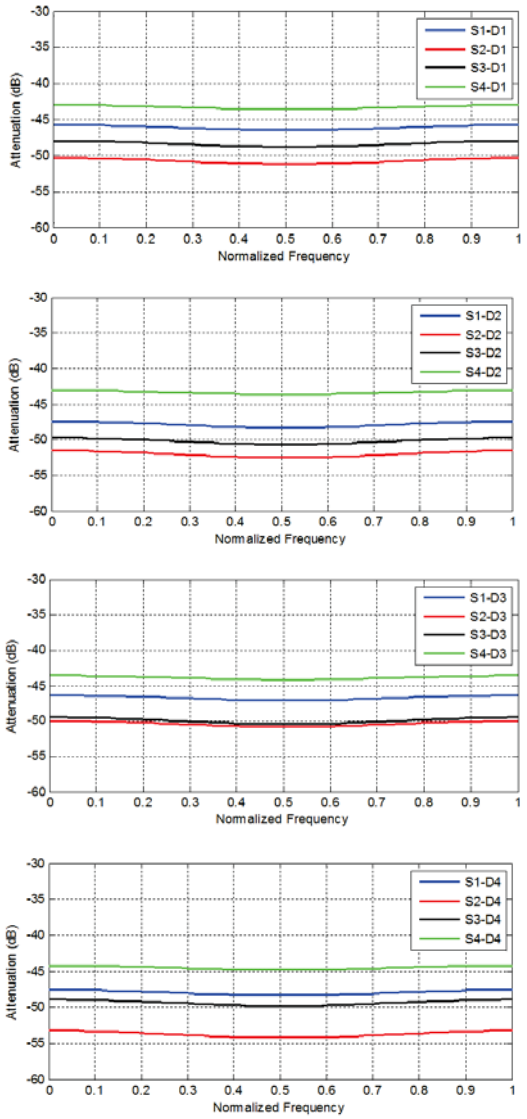

Fig. 3: Channel frequency responses for configuration C

and $N_{l,k}$ denote the kth positive and negative frame at layer l, respectively. In other words, $P_{l,k}$ and $N_{l,k}$ are generated from the kth bipolar OFDM frame of the corresponding layer. At the first layer ($l = 1$), 2^{L-1} U-OFDM frames are generated and concatenated to obtain the main frame of layer 1. At the second layer, 2^{L-2} U-OFDM frames are generated but positive and negative frames are replicated twice before forming the main frame of this layer. A similar procedure is applied at layer 3 but the corresponding frames are replicated four times for this layer. For the lth layer, each unipolar frame is replicated 2^{l-1} times according to eU-OFDM principle. After the formation of L main frames, these frames are added and used to modulate the intensity of an LED.

At the receiver side, due to the appropriate replication of the U-OFDM frames of the lower layers, the interference of the U-OFDM frames at the lower layers to the U-OFDM frames at a higher layer is eliminated. As an example, for layer 1, each negative frame is subtracted from each positive frame, and the corresponding bipolar frame is obtained. Please note that the structure of eU-OFDM eliminates the interference from lower layers to layer 1 as seen from Fig. 7. After demodulation of the information bits, these bits are modulated again to obtain the main frame of layer 1 and this frame is subtracted from the overall received signal to remove the interference of the signals of these layer to the lower layers. This iterative demodulation procedure continues for other layers [6]. Due to its improved spectral and energy efficiencies, eU-OFDM appears as a strong alternative to DCO-OFDM. It is shown in [15] that by considering $D = 5$, the spectral efficiency of eU-OFDM reaches 96.8% as that of DCO-OFDM ($\eta_D = \log_2(M)/2$).

Due to the advantages of MIMO transmission techniques, the combination of MIMO and eU-OFDM appears as a promising optical OFDM solution. In Fig. 8, the block diagram of the proposed MIMO-eU-OFDM scheme is presented. In this scheme, eU-OFDM is combined with V-BLAST technique, and considering an optical MIMO system of T LEDs and R PDs, each LED transmits its own eU-OFDM signals to improve the overall throughput of the system. Therefore, the spectral efficiency of the proposed scheme becomes

$$\eta_{new} \approx \frac{T \log_2(M)}{2}. \tag{4}$$

Denoting the vector of transmitted signals in a time instance by $\mathbf{x} \in \mathbb{R}^{T\times 1}$, the received signals $\mathbf{y} \in \mathbb{R}^{R\times 1}$ can be given as

$$\mathbf{y} = \mathbf{H}\mathbf{x} + \mathbf{n} \tag{5}$$

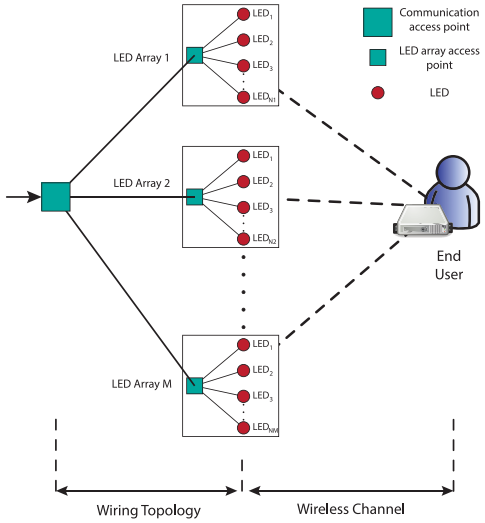

Fig. 4: Wiring topology between communication access point and luminaries

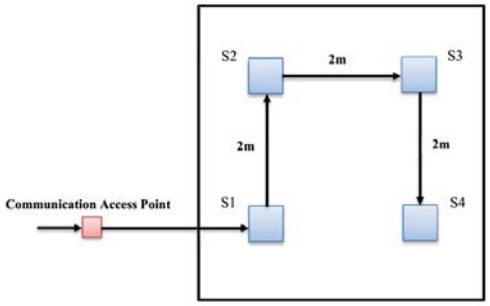

Fig. 5: Cabling topology in configuration C via CAT-5

where $\mathbf{H} \in \mathbb{R}^{R\times T}$ is the channel matrix whose elements are shown in Table I for $T = R = 4$, and $\mathbf{n}$ is the noise vector.

At the receiver side, the interference between the signals transmitted from different LEDs is eliminated by a zero-forcing (ZF) detector, i.e., $\mathbf{z} = \mathbf{H}^{-1}\mathbf{y}$, and each eU-OFDM frame is demodulated in a successive interference cancellation way as in [6]. For the evaluation of the error performance, we consider the average received electrical signal-to-noise ratio (SNR) as [16]

$$SNR = \frac{P_{Rx}^{E}}{\sigma_n^2} = \frac{1}{\sigma_n^2}\left(\frac{1}{R}\sum_{r=1}^{R}\sum_{t=1}^{T} h_{r,t} I\right)^2 \quad (6)$$

where P_{Rx}^{E} is the average received electrical power, σ_n^2 is the power of the Gaussian noise samples, I is the mean optical intensity (average optical power of eU-OFDM), which is calculated as

$$I = \frac{1}{\sqrt{2\pi}}\sum_{l=1}^{L}\frac{1}{\sqrt{2^{d-1}}} \quad (7)$$

where unit-energy time-domain signals are considered and the amplitude of the frames at layer l is scaled by $1/\sqrt{2^{d-1}}$.

IV. Computer Simulation Results

In this section, we provide computer simulation results for the proposed MIMO-eU-OFDM scheme for realistic indoor optical wireless channels. The BER performance

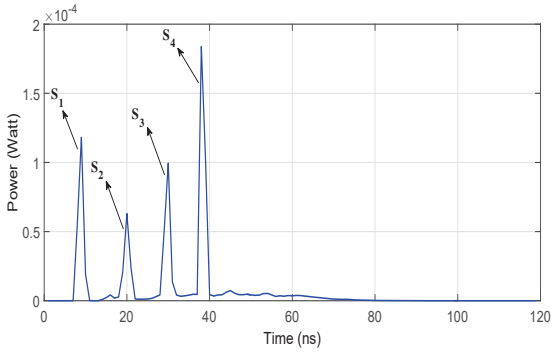

Fig. 6: Channel impulse response for configuration C including the delays caused by cabling

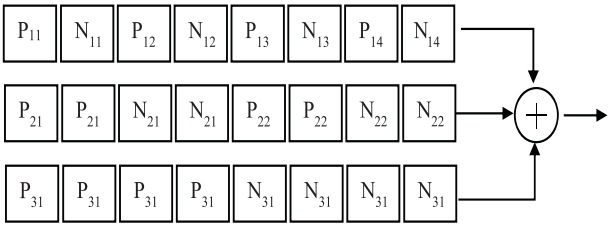

Fig. 7: eU-OFDM signal generation for $L = 3$ layers

of the proposed scheme is compared with V-BLAST-DCO-OFDM scheme which extends the concept of DCO-OFDM to MIMO systems [7]. For the considered signal constellation, the DC bias value [4] is set as 7 dB for DCO-OFDM. Two MIMO setups are considered: 2×2 and 4×4. Three different configurations (configurations A, B and C) given in Table I are considered. For 4×4 MIMO channel, the channel coefficients of Table I are used, while for 2×2 MIMO case, we considered the elements correspond to first and third columns and rows of the channel matrix of the 4×4 case. The number of OFDM subcarriers is taken as $N_{FFT} = 128$ and 4-QAM constellation is considered. Number of layers are selected as $L = 5$ for the MIMO-eU-OFDM scheme and ZF detector is used at the receiver. In Fig. 9, the BER performance of the MIMO-eU-OFDM and V-BLAST-DCO-OFDM schemes are given for a 2×2 MIMO system with configurations A, B and C where 2 bits/sec/Hz of spectral efficiency is obtained for both systems. As seen from Fig. 9, the proposed MIMO-eU-OFDM scheme achieves a better BER performance than the V-BLAST-DCO scheme for all considered configurations. In Fig. 10, we compare the BER performance of the MIMO-eU-OFDM and V-BLAST-DCO-OFDM schemes for a 4×4 MIMO setup with configurations A, B and C where 4 bits/sec/Hz of spectral efficiency is obtained for both systems. Similar to 2×2 case, the proposed scheme outperforms the reference scheme for all configurations.

It is interesting to note that due to the structure of the channel matrix with highly correlated elements, the performance of the considered schemes get worse for the 4×4 MIMO system as well as the BER performances of the systems for configurations A and C are worse than the BER performance for configuration B. However, the spectral efficiency is doubled without increasing the constellation size for the 4×4 MIMO system. On the other hand, the results of Figs. 9-10 give insight for the design of future OWC setups, which requires channel matrices with lower correlation among their elements to obtain better BER performance.

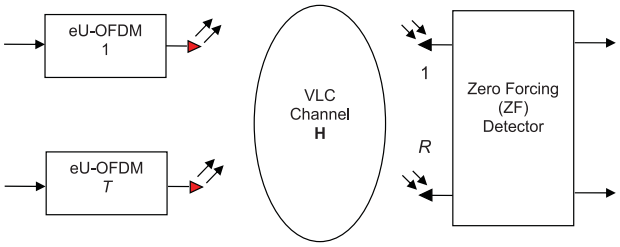

Fig. 8: MIMO-eU-OFDM system model for $T \times R$ Optical MIMO System

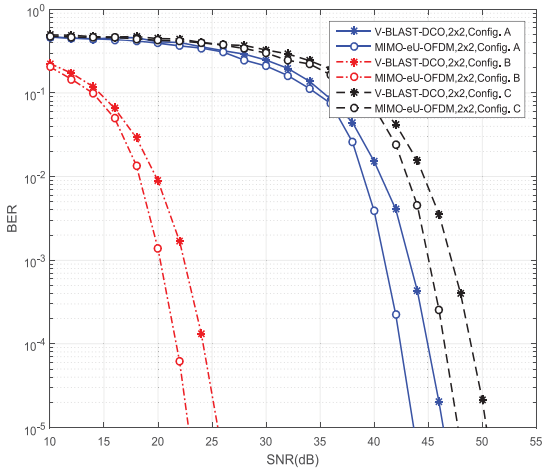

Fig. 9: Performance of MIMO-eU-OFDM and V-BLAST-DCO-OFDM for 2×2 MIMO system

V. Conclusions

In this paper, first, realistic indoor MIMO-VLC channel characterization and modeling were investigated by a non-sequential ray tracing approach. Indoor VLC CIRs for different MIMO configurations and scenarios were considered by taking some practical challenges into account such as number of LED chips per luminary, spacing between LED chips, objects inside the room and cabling topology. In particular, our results have demonstrated that the wiring topology should be taken into consideration to evaluate the CIRs. Our results have further shown that the CIR in an indoor environment including the propagation delays caused by wiring leads to a frequency selective sparse channel structure.

Second, by combining the eU-OFDM scheme and MIMO transmission techniques, a new VLC system, called MIMO-eU-OFDM was proposed and its BER performance was investigated in the presence of 2×2 and 4×4 realistic indoor MIMO-VLC channels. It was concluded that due to the structure of the channel matrix with highly correlated elements, the performance of the considered schemes has gotten worse for the 4×4 MIMO system. Particularly, we concluded that the BER performances of the systems for configurations A and C are worse than that of the configuration B. However, the spectral efficiency was doubled without increasing the constellation size for the 4×4 MIMO system. Consequently, the performance results obtained in the paper have given insight for the design of future OWC setups, which requires channel matrices with lower correlation among their elements to obtain better BER performance.

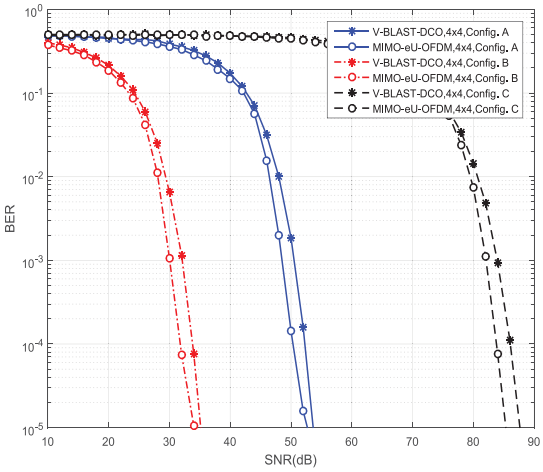

Fig. 10: Performance of MIMO-eU-OFDM and V-BLAST-DCO-OFDM for 4×4 MIMO system

References

[1] H. Haas, "High-speed wireless networking using visible light," *SPIE Newsroom*, Apr. 2013.

[2] T. Lee and A. Dentai, "Power and modulation bandwidth of GaAs-AlGaAs high-radiance LED's for optical communication systems," *Quantum Electronics, IEEE Journal of*, vol. 14, pp. 150–159, Mar. 1978.

[3] J. Armstrong, "OFDM for optical communications," *Lightwave Technology, Journal of*, vol. 27, pp. 189–204, Feb. 2009.

[4] S. Dissanayake and J. Armstrong, "Comparison of ACO-OFDM, DCO-OFDM and ADO-OFDM in IM/DD systems," *Lightwave Technology, Journal of*, vol. 31, pp. 1063–1072, Apr. 2013.

[5] D. Tsonev, S. Sinanovic, and H. Haas, "Novel unipolar orthogonal frequency division multiplexing (U-OFDM) for optical wireless," in *Vehicular Technology Conference (VTC Spring), 2012 IEEE 75th*, pp. 1–5, May 2012.

[6] D. Tsonev and H. Haas, "Avoiding spectral efficiency loss in unipolar OFDM for optical wireless communication," in *Communications (ICC), 2014 IEEE International Conference on*, pp. 3336–3341, June 2014.

[7] T. Fath and H. Haas, "Performance comparison of MIMO techniques for optical wireless communications in indoor environments," *Communications, IEEE Transactions on*, vol. 61, pp. 733–742, Feb. 2013.

[8] "Zemax 13 Release 2, Radiant Zemax LLC [Online]." http://www.zemax.com. Accessed: 09-02-2016.

[9] E. Sarbazi, M. Uysal, M. Abdallah, and K. Qaraqe, "Indoor channel modelling and characterization for visible light communications," in *Transparent Optical Networks (ICTON), 2014 16th International Conference on*, pp. 1–4, July 2014.

[10] F. Miramirkhani, M. Uysal, and E. Panayirci, "Novel channel models for visible light communications," in *Proc. SPIE*, vol. 9387, pp. 93870Q–93870Q–13, 2015.

[11] F. Miramirkhani and M. Uysal, "Channel modeling and characterization for visible light communications," *Photonics Journal, IEEE*, vol. 7, pp. 1–16, Dec. 2015.

[12] K. Lee, H. Park, and J. Barry, "Indoor channel characteristics for visible light communications," *Communications Letters, IEEE*, vol. 15, pp. 217–219, Feb. 2011.

[13] J. Ding, K. Wang, and Z. Xu, "Impact of LED array simplification on indoor visible light communication channel modeling," in *Communication Systems, Networks Digital Signal Processing (CSNDSP), 2014 9th International Symposium on*, pp. 1159–1164, July 2014.

[14] R. Kizilirmak and M. Uysal, "Single color networks: OFDM-based visible light broadcasting," in *Computer, Communications, and Control Technology (I4CT), 2015 International Conference on*, pp. 544–549, Apr. 2015.

[15] D. Tsonev, S. Videv, and H. Haas, "Unlocking spectral efficiency in intensity modulation and direct detection systems," *Selected Areas in Communications, IEEE Journal on*, vol. 33, pp. 1758–1770, Sept. 2015.

[16] R. Mesleh, H. Elgala, and H. Haas, "Optical spatial modulation," *Optical Communications and Networking, IEEE/OSA Journal of*, vol. 3, pp. 234–244, Mar. 2011.